JOURNAL OF APPLIED ELECTROCHEMISTRY 6 (1976) 229–235

*The electrolytic reduction of chalcopyrite in acid solution**

T. BIEGLER, D. A. SWIFT

CSIRO Division of Mineral Chemistry, P.O. Box 124, Port Melbourne, Victoria 3207, Australia

Received 25 April 1975

Chalcopyrite electrodes of both natural and synthetic material were cathodically reduced in several acid electrolytes. At current densities below 10 mA cm^{-2} chalcocite was formed and at higher currents the solid product contained elemental copper. The other reduction products were H_2S and Fe^{++}. The current efficiency, measured in terms of the Fe^{++} produced, generally fell with the amount of charge passed, the extent of the decrease depending on current density and the composition and temperature of the electrolyte. The decrease was attributed to evolution of hydrogen on the increasing surface area of the porous solid product as a consequence of inhibition of the chalcopyrite reduction process by ferrous salt precipitated in the pores. At sufficiently low current densities and short periods of electrolysis, chalcopyrite reduction was found to be activation controlled over a three order of magnitude range of currents, with a Tafel slope consistent with a one electron rate-determining step.

1. Introduction

Chalcopyrite, $CuFeS_2$, the most important economic source of copper, is a semiconducting mineral (generally *n*-type) which, like other conducting sulphides, can be electrolytically decomposed. The interest in the electrochemistry of such minerals (see e.g. [1]) stems largely from the fact that many sulphides can be anodically oxidized yielding the metal in solution and a residue of elemental sulphur, thereby allowing direct electrowinning of metals from their ores in a single electrolysis stage. A major nickel refining process is based on this principle [2]. Somewhat less attention has been paid to cathodic processes of metal sulphides, although there is a possibility that electrolytic reduction, which can yield other sulphide phases or even the metal, might also prove to be of interest in mineral processing.

Thermodynamic data for chalcopyrite, summarized in the form of E_h-pH diagrams [3, 4], predict that in solutions of pH around zero the copper-containing solid phases found at equilibrium at progressively decreasing potentials are, in order, chalcopyrite, bornite (Cu_5FeS_4), chalcocite (Cu_2S) and elemental copper. The stability boundaries between these phases are all below the reversible hydrogen potential, which means that their actual formation will depend on kinetic factors, in particular the overpotential for hydrogen evolution. Majima and Peters, in an unpublished report [5] mention experiments in which chalcopyrite was reduced in 1 M $HClO_4$ at a current density of 8 mA cm^{-2} (potential about −0·3 V versus S.H.E.), yielding hydrogen sulphide and ferrous ion in the molar ratio 3 : 2 and a solid product containing both bornite and chalcocite. These results were claimed to be consistent with the occurrence of both of the reactions

$$2CuFeS_2 + 6H^+ + 2e \rightarrow Cu_2S + 3H_2S + 2Fe^{++} \quad (1)$$

$$5CuFeS_2 + 12H^+ + 4e \rightarrow Cu_5FeS_4 + 6H_2S + 4Fe^{++}. \quad (2)$$

A negligible quantity of hydrogen was evolved.

Because of the possible relevance of these reactions to the development of new hydrometallurgical processes for copper extraction, in particular the activation of chalcopyrite by electrolysis of a slurry of copper concentrate [6], we have carried out a detailed study of the reduction of chalcopyrite, with emphasis on the factors which determine the current efficiency.

2. Experimental

Both natural and synthetic chalcopyrite were used in electrolysis experiments. Several rectangular

---

* Presented in part at the 102nd Annual Meeting, AIME, Chicago, 1973.

blocks (about 1 x 1 x 1·5 cm) of natural material were cut from each of two massive specimens of chalcopyrite, one from Moonta Mines, South Australia, and the other from an unknown location. Both specimens were *n*-type with resistivities of 3–4 Ω cm. A threaded brass contact was attached to the block by means of a conducting epoxy adhesive (Epo-tek 410E, Epoxy Technology Inc., Watertown, Mass., U.S.A.) and the assembly embedded in epoxy mounting resin (Araldite D, CIBA) leaving the threaded opening clear for insertion of a stainless steel contact rod. An electrode surface of well-defined area was exposed by grinding the resin from the face furthest from the electrical contact. Surface renewal by grinding was carried out after each run.

Synthetic chalcopyrite was prepared by a method similar to that described by Dutrizac and MacDonald [7] but modified to provide a less porous product. Covellite (CuS) and troilite (FeS), each synthesized from the elements, were ground, screened, mixed in stoichiometric quantities and reacted together under pressure (1·5 kbar) in a heated die (510° C) for 1 h. The material so produced was ground, mixed and sintered again (1·5 kbar, 450° C, 30 min) to give thin slabs (approximately 2 x 1 x 0·3 cm) suitable for use as electrodes. This procedure gave a massive product (S.G. 4·1–4·2, *cf.* theoretical for chalcopyrite 4·088) which, by mineragraphic examination, X-ray diffraction and electron microprobe analysis, was shown to be substantially chalcopyrite. However, as is to be expected from the complexity of phase relations known to exist in this system [8], minor inclusions of other phases were present; bornite, pyrite, γ-chalcopyrite [8], and the primitive cubic phase [8] were identified by electron microprobe analysis. Electrical contact with synthetic electrodes was by means of a spring-loaded lead clip, lead being chosen for its inertness and high hydrogen overvoltage. These electrodes were only partly immersed in the electrolyte.

The electrolysis cell was a five-necked flange-topped glass vessel of total capacity 250 ml. A counter-electrode compartment (closed with a sintered glass disc), reference-electrode probe, gas inlet, gas outlet and working electrode were inserted through the necks. Most experiments were carried out in 2 M H_2SO_4 at 20° C and, unless otherwise indicated, these were the conditions used. The solution was purged with nitrogen at a rate of 120 ml min^{-1}. The reference electrode was either an S.C.E. or a mercury/mercurous sulphate, 1 M H_2SO_4 electrode whose potential was 0·43 V versus S.C.E. Potentials are quoted with respect to the S.H.E. (−0·244 V versus S.C.E.).

Galvanostatic experiments were performed with a Keithley model 225 constant current source and the potential recorded with a Hewlett Packard model 7100B strip chart recorder. A Wenking model 68TS3 potentiostat was used for controlled potential runs.

The course of the electrode reaction was followed by microscopic examination of the solid products in polished section, X-ray diffractometry of the products, either *in situ* or scraped from the surface, and chemical analysis of dissolved ferrous iron and hydrogen sulphide evolved. The latter was absorbed in ammonia and determined by precipitation of As_2S_3 from sodium arsenite and back-titration of excess arsenite with iodine. The solid product was weighed after removal from the electrode surface; scraping and brushing achieved good separation from the unreacted chalcopyrite. Iron was determined by atomic absorption spectroscopy. It was assumed that any charge not accountable in terms of the quantity of chalcopyrite reduced was consumed in the hydrogen evolution reaction.

3. Results and discussion

3.1. *Solid products of chalcopyrite reduction*

Chalcopyrite electrodes reduce fairly uniformly to give an adherent product layer which, when dried, is friable and easily removed. In these respects, natural and synthetic material behave similarly except that at higher current densities (> 10 mA cm^{-2}) the latter tends to shed a small amount of product mixed with some unreacted chalcopyrite. The nature of the solid product depends on the current density. Below about 10 mA cm^{-2} the product is generally the grey copper sulphide, chalcocite, though in some runs the closely related sulphide djurleite ($Cu_{1.97}S$), distinguishable only by X-ray diffraction analysis, is found. Experimental evidence from anodic oxidation of copper sulphides indicates [9] that the standard free energies of formation of chalcocite and djurleite differ by only 1·2 kJ mol^{-1}. Using these standard free energies [9], we calculate that the standard potentials for the reactions forming chalcocite and djurleite from chalcopyrite are −0·138 and −0·144 V respectively, the close proximity of these values presumably allowing formation of the two sulphides under very similar conditions.

At higher current densities elemental copper is formed and becomes the major component of the product above 50 mA cm^{-2}. Since it is in a finely divided, reactive state, it oxidizes rapidly in air and is detected by X-ray diffraction as a mixture of copper and cuprous oxide. Examination of electrodes in section shows that copper forms at the solution side of the chalcocite layer, indicating that chalcocite is an intermediate in the reduction to copper. The reaction is therefore

$$Cu_2S + 2H^+ + 2e \rightarrow 2Cu^0 + H_2S \qquad (3)$$

for which the calculated standard potential, using the data for [9], is −0·269 V. Experimentally, copper appears when the potential reaches about −0·4 V.

Bornite is notably absent from any of the products of galvanostatic electrolysis, in contrast to the report of Majima and Peters quoted earlier. Since the supposed narrow region of bornite stability is anodic to the chalcocite domain [3, 4], it could be argued that bornite should form at lower currents or less cathodic potentials than were operating in the experiments described above. Accordingly, several potentiostatic runs at potentials between −0·05 and −0·2 V were carried out on polished electrodes (natural chalcopyrite) in epoxy mounts which could be directly inserted into the specimen chamber of the X-ray diffractometer. With this technique, thin product layers formed at low reaction rates could be identified without the need to scrape off the material. At −0·05 V, the current decays within a few minutes to less than 50 μA cm^{-2} and long periods (20 h) are needed to generate a detectable amount of product. In this case, as at more cathodic potentials, the product is found to contain only chalcocite. In a duplication of the experiment described by Majima and Peters [5] (1 M $HClO_4$, 8 mA cm^{-2}), once again only chalcocite is detected.

When the chalcocite is removed from a reduced electrode, the exposed surface tarnishes more rapidly than chalcopyrite, giving shades of pink, blue and purple. This observation raises the possibility that the reduction process occurs via an intermediate such as talnakhite ($Cu_9Fe_8S_{16}$) or mooihoekite ($Cu_9Fe_9S_{16}$), sulphides which are known to tarnish more rapidly than chalcopyrite [10]. Talnakhite, for example, could form according to the reaction

$$9CuFeS_2 + 4H^+ + 2e \rightarrow Cu_9Fe_8S_{16} + 2H_2S + Fe^{++} \qquad (4)$$

which clearly could be considered an intermediate step in the overall Reaction 1. Electron microprobe measurements have, however, failed to confirm the presence of an intermediate phase on the surface; scans for copper, iron and sulphur content in a direction normal to the reacted surface show a sharp jump to the values for chalcopyrite when the beam crosses the interface between chalcocite and apparently unreacted chalcopyrite. Any intermediate layer must therefore be thinner than the electron beam diameter, in this case about 5 μm.

3.2. *Stoichiometry of chalcocite formation*

At current densities of about 10 mA cm^{-2} and below, the sole presence of chalcocite in the products virtually assures that the reaction proceeds according to Equation 1, but as a further test the yields of iron, hydrogen sulphide and chalcocite are compared (Table 1) with those calculated from Equation 1, based on the quantity of chalcopyrite

Table 1. Product yields for reduction of synthetic chalcopyrite at 4 mA cm^{-2} in 2 M H_2SO_4

Run	*$CuFeS_2$ reacted* (10^{-3} mol)	*Cu_2S* (10^{-3} mol)		*H_2S* (10^{-3} mol)		*Fe^{++}* (10^{-3} mol)	
		Found	*Calculated*	*Found*	*Calculated*	*Found*	*Calculated*
1	10·5	5·2	5·2	14·1	15·7	9·9	10·5
2	6·1	3·2	3·1	7·8	9·2	5·9	6·1
3	6·3	3·1	3·1	8·0	9·4	6·6	6·3

consumed. Agreement is fair, with the major disparity being a low yield of hydrogen sulphide which we attribute to the difficulties in analysing small quantities in dilute gas streams. In subsequent discussion, iron entering solution is taken as the more reliable and easily determined measure of the extent of reaction.

3.3. *Current efficiency of chalcopyrite reduction*

Progressive measurements of iron dissolved as a function of charge passed are shown in Fig. 1. The scales are chosen to allow proper comparison of results for electrodes of different areas. At a given current density it can be seen that the rate of chalcopyrite reduction decreases with the extent of the reaction. After passage of a given amount of charge, the extent of reaction is smaller the higher the current density. At sufficiently low current densities, the rate of iron dissolution is, within experimental error, the same as that calculated from Equation 1 with a current efficiency of 100% (see broken line, Fig. 1).

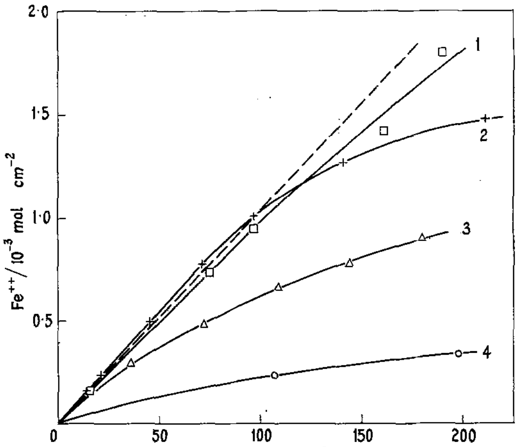

Fig. 1. Iron dissolution as a function of charge passed in reducing natural (curves 1, 3, 4) and synthetic (curve 2) chalcopyrite in 2 M H_2SO_4 at 20° C. Current densities are (1) 1·0; (2) 3·9; (3) 10; (4) 100 mA cm^{-2}. Broken line shows quantity of iron for Reaction 1 at 100% current efficiency.

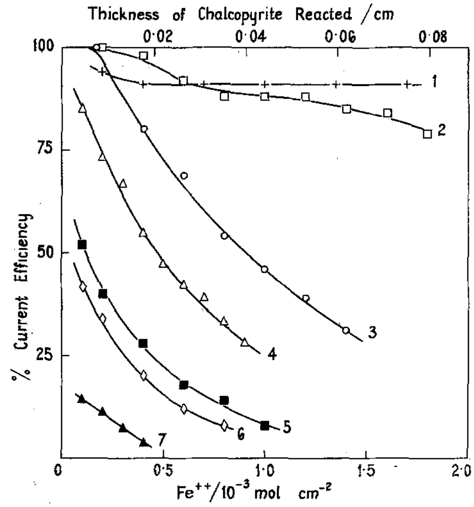

Fig. 2. Dependence of current efficiency for Reaction 1 or 1 + 3 (see text) on extent of reduction of natural chalcopyrite in 2 M H_2SO_4 at 20° C. Extent of reaction measured by iron dissolved per unit area (lower scale) or thickness of chalcopyrite reacted (upper scale), taking molar volume of chalcopyrite as 44·1 cm^3. Current densities are (1) 0·3; (2) 1·0; (3) and (4) 10; (5) 50; (6) 100; (7) 400 mA cm^{-2}.

The current efficiency at any stage is derived graphically by comparing the slope of the iron dissolution curve with the theoretical slope at 100% current efficiency of the appropriate reaction for chalcopyrite reduction. This procedure poses a problem whenever chalcocite is not the only solid product. In the absence of complete information concerning the proportions of chalcocite and copper formed at high current densities we have chosen to treat the results on the basis that the reaction involves one electron per Fe^{++} at 10 mA cm^{-2} and below (Equation 1) and two electrons per Fe^{++} at higher current densities (Equations 1 + 3). Current efficiencies calculated in this way are shown in Fig. 2 as functions of the extent of reaction, expressed in terms of either the iron dissolved or the equivalent thickness of chalcopyrite reacted. Being essentially differential curves, they are very sensitive to errors in the iron analyses and to the way in which the iron dissolution data are smoothed; an indication of the uncertainty involved is given by curves 3 and 4 (Fig. 2) which are the extreme results from several runs under similar conditions. Nevertheless, the results clearly show the general features of maintenance of high current efficiency at low current densities ($\leqslant 1$ mA cm^{-2}) and, at high current densities, a current efficiency which falls steeply with extent of reaction. Current efficiencies with synthetic chalcopyrite are the same as, or slightly lower than, with natural material.

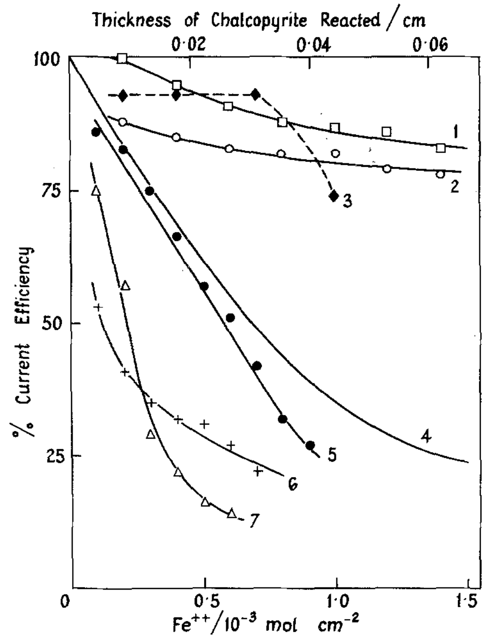

Fig. 3. Dependence of current efficiency on extent of reduction (see legend, Fig. 2) of natural chalcopyrite under various conditions; current density 10 mA cm^{-2}, except (3) 8 mA cm^{-2}. (1) 2 M H_2SO_4, 45 and 70° C; (2) 6 M HCl, 20° C; (3) 1 M $HClO_4$, 25° C; (4) 2 M H_2SO_4, 20° C (pooled data from several runs); (5) 2 M H_2SO_4 + 0·04 M $FeSO_4$, unpurged, 20°C; (6) 0·2 M H_2SO_4, 20° C; (7) 6 M H_2SO_4, 20° C.

Results of this kind were used to examine the effects of several factors on the course of reduction of chalcopyrite electrodes. A current density of 10 mA cm^{-2} was chosen for making comparisons under different conditions. In 0·6 M H_2SO_4, the current efficiency is similar to that in 2 M H_2SO_4 (Fig. 3, curve 4) but decreases at both lower (0·2 M, curve 6) and higher (6 M, curve 7) acid concentrations. Increase in temperature above 20° C has a significant effect in increasing current efficiency in 2 M H_2SO_4 (*cf.* curves 1 and 4, Fig. 3), though the experiments do not detect any difference between the behaviour at 45 and 70° C. When the electrolysis is conducted in the presence of additional ferrous ion in solution (0·04 M $FeSO_4$) and with accumulation of the H_2S produced (i.e. solution not purged), the current efficiency is not significantly affected except perhaps for a slight reduction towards the end of the run (Fig. 3, curve 5). In 6 M HCl, the current efficiency at 20° C is high (Fig. 3, curve 3) and is even greater at 70° C where it does not deviate significantly from 100% for reduction of up to 0·1 cm thickness of chalcopyrite. A high current efficiency is also found in 1M $HClO_4$ (Fig. 3, curve 3), consistent with the results of Majima and Peters [5].

Despite the progressive fall of current efficiency with time, the potential throughout runs such as represented in Fig. 2 remains constant within a few mV. It is therefore difficult to explain the increasing rate of hydrogen evolution in terms of a progressive decrease in potential. Furthermore, most of the current efficiency curves appear to extrapolate to initial values near 100%, suggesting that at these potentials the rate of hydrogen evolution on chalcopyrite itself is very small. The hydrogen evolution reaction therefore must occur on the surface of the reduction product, chalcocite, which remains electrically in contact with the electrode bulk. Since it is porous and flooded with electrolyte, this layer acts as an electrode of high surface area, roughly proportional to its thickness, while the chalcopyrite/electrolyte interfacial area remains relatively constant. Thus, even if the hydrogen overvoltage on chalcocite is no smaller than on chalcopyrite, the high ratio of the two areas could result in a significant rate of hydrogen evolution at the chalcocite surface.

The above considerations cannot alone account for the wide range of current efficiencies found under various conditions. In addition we need to suppose that the specific rates of the two basic reactions, reduction of chalcopyrite and hydrogen evolution on chalcocite (or copper), change by disproportionate amounts when the electrolysis conditions are changed. Though a number of factors can be suggested (e.g. different Tafel slopes, pH dependence, temperature coefficients or ion adsorption effects), we think the most important is likely to be solubility of ferrous ion in the electrolyte, and we propose that inhibition of the chalcopyrite reduction process results from precipitation of the iron salt at the chalcopyrite/electrolyte interface. When this occurs, the reduction rate becomes limited by diffusion of Fe^{++} through the pores within the chalcocite layer. This idea is consistant with the higher current efficiency attainable in HCl and $HClO_4$ media in which Fe^{++} is more soluble than in H_2SO_4 [11], with the marked effect of temperature in the latter medium and with the decline in current efficiency in 6 M

H_2SO_4 in which ferrous sulphate is only about 10% as soluble as in 2 M H_2SO_4 [11].

Support for the above mechanism can be obtained from calculation of surface Fe^{++} concentrations using a simple model in which constrained diffusion occurs within the porous product layer. If we make the approximation that the concentration gradient within that layer is uniform, the surface flux of Fe^{++}, and hence the current, are given by

$$i = FD\left(\frac{c_s - c_b}{\tau l}\right) \mathrm{A\,cm^{-2}} \tag{5}$$

where D is the diffusion coefficient of Fe^{++}, c_s and c_b the surface and bulk concentrations, l the thickness of product and τ is a tortuosity factor, typically 1·5–2 for an open porous solid [12], which gives the actual diffusion path length within the product pores. Under most experimental conditions $c_s \gg c_b$ so we can write

$$c_s = \frac{i\tau l}{FD} \mathrm{mol\,cm^{-3}}. \tag{6}$$

With $i = 10^{-2}\,\mathrm{A\,cm^{-2}}$, $\tau = 2$, $l = 10^{-2}$ cm and $D = 5 \times 10^{-6}\,\mathrm{cm^2\,s^{-1}}$ (taken as a value typical of a divalent cation at 20° C), the surface concentration of iron becomes 0·4 M and, of course, is proportionately greater as l or i increases. As a saturated solution of $FeSO_4$ in 2 M H_2SO_4 contains only about 0·6 M Fe^{++} at 20° C [11], it is easy to see that the solubility under the above conditions will be exceeded at chalcocite thicknesses of the order of 10^{-2} cm. This is well within the range encountered experimentally (Figs. 2 and 3) if we assume that the thicknesses of chalcocite formed and chalcopyrite reacted are about the same. Furthermore, it follows that the decreasing flux of Fe^{++} as l increases will contribute to the fall in current efficiency with extent of reaction found under most experimental conditions.

3.4. *Chalcopyrite reduction kinetics*

Fig. 4 shows a Tafel plot, determined galvanostatically, for natural chalcopyrite in 1 M $HClO_4$ at 25° C. This solution was selected because Reaction 1 occurs at, or close to, 100% current efficiency over the range of currents used, ensuring that the currents do indeed refer to this reaction. Data from experiments with a number of different electrodes in 2 M H_2SO_4 give a Tafel plot close to that of Fig. 4. Steady potentials are reached within a minute except below 0·1 $\mathrm{mA\,cm^{-2}}$ where 10–20 min are needed. There is good agreement between potentials recorded with decreasing and increasing currents, indicating that for the rather small total charge passed (~ 9 $\mathrm{C\,cm^{-2}}$) the potential is independent of the thickness of the product layer.

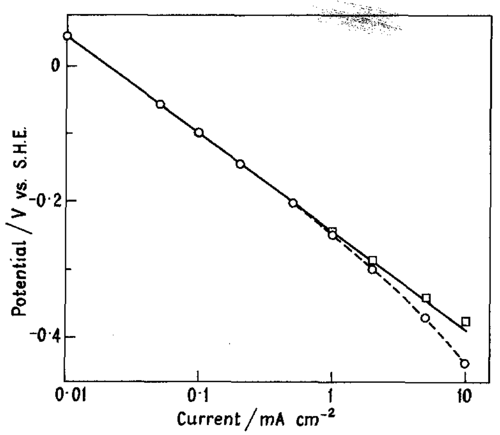

Fig. 4. Tafel plot for reduction of natural chalcopyrite in 1 M $HClO_4$ at 25°C. ○ measured potentials; □ potentials corrected for iR drop across 5 Ω electrode resistance.

The Tafel plot (Fig. 4) is linear except above 1 $\mathrm{mA\,cm^{-2}}$ where the deviations can be accounted for by a resistive voltage drop across an effective electrode resistance of 5 Ω. This value is in reasonable accord with separate resistance measurements made by means of a contact soldered to the working face of the electrode. Such measurements gave values ranging from 6–10 Ω depending on the position of the contact which covered only a small fraction of the electrode working area. The fact that the whole area is in contact with electrolyte during polarization measurements probably accounts for the lower effective resistance.

It is notable that the standard potential quoted previously for Reaction 1, −0·138 V, actually lies within the range covered in Fig. 4; at this potential the current is $2 \times 10^{-4}\,\mathrm{A\,cm^{-2}}$. The reaction is therefore quite fast, an unexpected result in view of the likely irreversibility of chalcopyrite reduction. It is improbable that chalcopyrite can be electrolytically generated through the reverse of Reaction 1, and our experimental attempts to achieve this reverse process have been unsuccessful. In these circumstances it would be meaningless to derive a value for exchange current from the data of Fig. 4.

The linearity of the Tafel plot and the lack of dependence of potential on the product layer thickness show that the reaction is under activation control. The Tafel slope of -144 mV is consistent with a one-electron rate-determining step and suggests a mechanism in which the slow step is the initial acceptance of an electron into the chalcopyrite lattice, perhaps at the Fe^{+++} site which Mössbauer studies [13] have shown to exist. This step is followed by rapid breakdown of the lattice, with dissolution of iron and sulphur and rearrangement of the remaining copper and sulphur atoms to give the copper sulphide product.

Anodic reactions of certain metal sulphides (e.g. Cu_2S) involve only dissolution of the metal, in which case there is the possibility that solid state diffusion of metal atoms plays a part in the mechanism (e.g. [14]). In the present reaction, the involvement of sulphur, generally considered to have low mobility in sulphide lattices, makes such a diffusion mechanism most unlikely except over very short distances (a few atomic diameters) or in the case of formation of a layer of a metal-deficient intermediate product essentially retaining the chalcopyrite sulphur lattice; as mentioned earlier, if such a layer exists it is not detected by electron microprobe analysis. The evidence therefore indicates that reduction of chalcopyrite can occur only at, or very close to, the interface between chalcopyrite and the electrolyte. The fact that the reaction interface can progress to a considerable depth is doubtless a consequence of the very porous nature of the solid product layer. Chalcocite occupies only about one-third of the volume of the chalcopyrite from which it forms and this shrinkage ensures that there is continued exposure to the electrolyte of fresh chalcopyrite surface.

References

[1] F. Habashi, *Miner. Sci. Eng.*, 3 (1971) 3.

[2] L. S. Renzoni, R. C. McQuire and M. V. Barker, *J. Metals* 10 (1958) 414.

[3] R. M. Garrels and L. Christ, 'Solutions, Minerals and Equilibria', Harper and Row, New York (1965).

[4] E. Peters and H. Majima, 'The physical chemistry of leaching of sulphide minerals', paper presented at 97th Annual Meeting AIME, New York (1968).

[5] H. Majima and E. Peters, 'Electrochemical mechanisms for the decomposition of metal sulphides', unpublished report.

[6] T. Biegler and D. C. Constable, 'Upgrading and activation of chalcopyrite concentrates by slurry electrolysis', to be published.

[7] J. E. Dutrizac and R. J. C. MacDonald, *Mat. Res. Bull.* 8 (1973) 961.

[8] L. J. Cabri, *Econ. Geol.* 68 (1973) 443.

[9] H. J. Mathieu and H. Rickert, *Z. Phys. Chem. (Frankfurt am Main)*, 79 (1972) 315.

[10] L. J. Cabri and S. R. Hall, *Amer. Mineral.* 57 (1972) 689.

[11] W. F. Linke, 'Solubilities of Inorganic and Metal-Organic Compounds', 4th edn. American Chemical Society, Washington (1958).

[12] C. N. Satterfield and T. K. Sherwood, 'The Role of Diffusion in Catalysis', Addison-Wesley, Reading, Mass. (1963).

[13] N. N. Greenwood and H. J. Whitfield, *J. Chem. Soc. A.* (1968), 1697.

[14] P. Brennet, S. Jafferali, J. Vanseveren, J. Vereecken and R. Winand, *Met. Trans.* 5 (1974) 127.